A Pile-up Model for Dispersed Spectra

John E. Davis

Center for Space Research
Massachusetts Institute of Technology
Cambridge, MA 02139

ABSTRACT

The observation of a bright X-ray source by the Chandra X-ray Observatory's High Energy Transmission Grating Spectrometer (HETGS) can be compromised by photon pile-up in the CCD leading to false absorption features in the observed spectrum. A method for removing the effects of pile-up in a dispersed grating spectrum is presented. The effectiveness of the technique is demonstrated through its application to the HETGS observation of 4U 1636-53, a bright X-ray binary system.

Keywords: Pile-up, Chandra, X-ray, Spectroscopy

1. INTRODUCTION

Pile-up is a consequence of the finite spatial and temporal resolution of a Charge Coupled Device (CCD), and will occur when two or more photons participate in the same spatial and temporal resolution element. In such a case, the detector will be unable to separately resolve the individual photons causing the ensuing event to have a pulse-height (PHA) that is roughly the sum of the pulse-heights of the individual photon events in the absence of pile-up. As a result, pile-up lowers the event detection rate and distorts the observed CCD PHA spectrum towards higher energies.

A general method for correcting for CCD pile-up was previously given by the author.[1] However that work was not taylored to the specific case of pile-up of dispersed spectra. The goal of the current paper is to formulate a pile-up model that is applicable to dispersive spectroscopy.

In the next section, the standard technique for the analysis of dispersed data not affected by pile-up is reviewed. This section also serves to describe the notation and conventions used throughout this paper. The formulation of the dispersive pile-up model follows in section 3. The effectiveness of the model is demonstrated in section 4 through its application to a Chandra X-ray Observatory[2] observation of 4U 1636-53, a bright X-ray binary system. The paper is concluded in section 5 with a brief summary of the results of this work.

2. STANDARD ANALYSIS FORMALISM

This section provides a review of the standard technique for "flux-correcting" grating data in the absence of pile-up effects.

The most fundamental equation of diffraction physics is the so-called grating equation,

$$m\lambda = p\sin\theta, \tag{1}$$

which relates the diffraction angle θ and the period p of the grating to the diffraction order m and wavelength λ of the diffracted photon. The above equation applies only to an ideal grating— one that is only approximately achieved in nature. For a realistic grating, the diffraction process must be characterized by a probability distribution that gives the probability for a diffracted photon of wavelength λ to have a direction in a specified solid angle. Such a distribution is described below.

Rather than working in the natural (x, y) pixel coordinate system of the detector, it is preferable to use a coordinate system that is better suited for the description of diffracted events. Hence, locations on the detector

Further author information: Send correspondence to J.E.D.: E-mail: davis@space.mit.edu, Telephone: 617-258-8119

X-Ray and Gamma-Ray Telescopes and Instruments for Astronomy, Joachim E. Trümper, Harvey D. Tananbaum, Editors, Proceedings of SPIE Vol. 4851 (2003)

will be given in terms of a dispersion coordinate θ and a cross-dispersion coordinate z. The origin of (θ, z) system is taken to be at the mean position for zeroth order events. Instead of using angular units for θ, *wavelength units will be used by scaling the angular units by the grating period p*. This choice of units eliminates p from many of the subsequent equations, and has the feature that θ corresponds to the first-order wavelength scale. Assuming small angles, the grating equation can be expressed in these units as

$$m\lambda = \theta. \tag{2}$$

In this coordinate system, the normalized probability distribution described above can be written as

$$\mathcal{G}^{(m)}(\theta, z, \lambda)\mathrm{d}\theta\, \mathrm{d}z, \tag{3}$$

which gives the probability for an mth order diffracted photon with wavelength λ to intersect the detector at a dispersion coordinate between θ and $\theta + \mathrm{d}\theta$, and a cross-dispersion coordinate between z and $z + \mathrm{d}z$. For a fixed wavelength λ, the distribution $\mathcal{G}^{(m)}(\theta, z, \lambda)$ is strongly peaked about $z = 0$ and the value of θ satisfying the grating equation, i.e., $\theta = m\lambda$.

Important related quantities are the Line Spread Function (LSF) and the cross-dispersion Encircled Energy Fraction (EEF). The mth order cross-dispersion EEF for the region between z_1 and z_2 is defined as

$$f^{(m)}(\lambda; z_1, z_2) = \int_{-\infty}^{\infty} \mathrm{d}\theta \int_{z_1}^{z_2} \mathrm{d}z\, \mathcal{G}^{(m)}(\theta, z, \lambda). \tag{4}$$

The LSF for this region is defined as

$$\mathcal{L}(\theta, \lambda; z_1, z_2) = \frac{1}{f^{(m)}(\lambda; z_1, z_2)} \int_{z_1}^{z_2} \mathrm{d}z\, \mathcal{G}^{(m)}(\theta, z, \lambda), \tag{5}$$

and by construction, satisfies the normalization condition

$$1 = \int_{-\infty}^{\infty} \mathrm{d}\theta \mathcal{L}(\theta, \lambda; z_1, z_2). \tag{6}$$

In several places throughout this paper integrals of the form

$$\int \mathrm{d}\lambda \int_{\theta - \Delta\theta/2}^{\theta + \Delta\theta/2} \mathrm{d}\theta' \int_{z_1}^{z_2} \mathrm{d}z\, \mathcal{G}^{(m)}(\theta', z, \lambda) \tag{7}$$

will be encountered. Such integrals can written in terms of the EEF by observing that if $\Delta\theta$ is small, then because of the sharpness of $\mathcal{G}^{(m)}(\theta', z, \lambda)$, only a narrow range of wavelengths near θ/m will actually contribute to the integral. For this small range, the function $\mathcal{G}^{(m)}(\theta, z, \lambda)$ may be assumed to be translation-invariant such that it can be regarded as a function of $\theta - \lambda$, i.e., $\mathcal{G}^{(m)}(\theta - \lambda, z)$. By making the appropriate change of variables, it is easy to show the equality

$$f^{(m)}(\theta/m; z_1, z_2)\Delta\theta = \int \mathrm{d}\lambda \int_{\theta}^{\theta + \Delta\theta} \mathrm{d}\theta' \int_{z_1}^{z_2} \mathrm{d}z\, \mathcal{G}^{(m)}(\theta', z, \lambda). \tag{8}$$

Now consider a point source with a spectrum $s(\lambda)$ defined such that $s(\lambda)\mathrm{d}\lambda$ gives the number of photons per cm^2 per second with wavelengths between λ and $\lambda + \mathrm{d}\lambda$ incident upon the telescope. Suppose that events from such a source are extracted from a rectangular region (in diffraction coordinates) with a cross-dispersion width w centered upon $z = 0$, and with the dispersion coordinate θ binned in units of $\Delta\theta$. Let Ω_i denote the ith such bin, i.e., the bin containing events with $i\Delta\theta \le \theta < (i + 1)\Delta\theta$ and $-w/2 \le z < w/2$. In the absence of pile-up, the expected number of events in this bin with pulse-height h is given by

$$C_{\Omega_i}(h) = \sum_m C_{\Omega_i}^{(m)}(h), \tag{9}$$

where[3]

$$C_{\Omega_i}^{(m)}(h) = (N\tau) \int \mathrm{d}\lambda \; G_{\Omega_i}^{(m)}(\lambda) A^{(m)}(h,\lambda) s(\lambda), \tag{10}$$

and

$$G_{\Omega_i}^{(m)}(\lambda) = \int_{i\Delta\theta}^{(i+1)\Delta\theta} \mathrm{d}\theta \int_{-w/2}^{w/2} \mathrm{d}z \; \mathcal{G}^{(m)}(\theta, z, \lambda). \tag{11}$$

Here, $C_{\Omega_i}^{(m)}(h)$ represents the mth order diffracted "counts" spectrum, which gives the number of mth order events with pulse-height h expected in the ith bin. The quantity $A^{(m)}(h,\lambda)$ represents the effective area associated with a photon of wavelength λ diffracted into the mth order to produce an event with pulse-height h. The total exposure time is given by $(N\tau)$, where N represents the number of CCD frames, and τ is the CCD frame-time, i.e., the time of each individual CCD frame.

If the CCD has enough intrinsic energy resolution as does a Chandra ACIS CCD, and the bins Ω_i are small enough, one could exploit the correlation between the pulse-height of an event and the energy of the incident photon to extract mth order events from a bin. Call the total number of such events $C_{\Omega_i}^{(m)}$. Also denote $A^{(m)}(\lambda)$ to be the effective area modified by the pulse-height filter implied by this order-sorting process.[3] The relationship between these quantities may be written as

$$C_{\Omega_i}^{(m)} = (N\tau) \int \mathrm{d}\lambda \; G_{\Omega_i}^{(m)}(\lambda) A^{(m)}(\lambda) s(\lambda). \tag{12}$$

Owing to the strongly peaked nature of $G_{\Omega_i}^{(m)}(\lambda)$, for a specified region Ω_i and an order m, only a narrow range of wavelengths near the value satisfying the grating equation will contribute to the integral. If the range of wavelengths for mth order photons falling into the ith bin has a width of $\Delta\lambda_i^{(m)}$, then the above integral may be written

$$C_{\Omega_i}^{(m)} = (N\tau) \int_{\lambda_i^{(m)} - \Delta\lambda_i^{(m)}/2}^{\lambda_i^{(m)} + \Delta\lambda_i^{(m)}/2} \mathrm{d}\lambda \; G_{\Omega_i}^{(m)}(\lambda) A^{(m)}(\lambda) s(\lambda), \tag{13}$$

where

$$\lambda_i^{(m)} = (i + \frac{1}{2}) \frac{\Delta\theta}{m} \tag{14}$$

denotes the wavelength of an mth order photon at the center of the ith bin. Now, if $\Delta\lambda_i^{(m)}$ is small such that $s(\lambda)$ does not vary much over the integration region, then it may be approximated by its average value in the interval, written here as $\bar{s}_i^{(m)}$. This procedure yields the *flux-corrected* spectrum

$$\bar{s}_i^{(m)} = \frac{C_{\Omega_i}^{(m)}}{(N\tau) \int \mathrm{d}\lambda \; G_{\Omega_i}^{(m)}(\lambda) A^{(m)}(\lambda)}. \tag{15}$$

This equation may be put in a more familiar form by assuming that the effective area does not vary much over the interval $\Delta\lambda_i^{(m)}$, then it too may be replaced by its average value over the region and removed from the integral. Then using Eq. 8, it follows that

$$\bar{s}_i^{(m)} = \frac{C_{\Omega_i}^{(m)}}{(N\tau) A_i^{(m)} f_i^{(m)} \Delta\theta}, \tag{16}$$

where $A_i^{(m)} = A^{(m)}(\lambda_i^{(m)})$ and $f_i^{(m)} = f^{(m)}(\lambda_i^{(m)}; -w/2, w/2)$.

The linearity of equations (15) and (16) is a reflection of the assumption that $s(\lambda)$ is small enough that pile-up can be neglected. In the next section, a modification to Eq. 16 will be presented that takes into account the effects of pile-up.

3. A DISPERSIVE PILE-UP MODEL

As mentioned above, pile-up is a consequence of the limited spatial and temporal resolution of the CCD. Correcting for the effects of pile-up requires consideration of these limiting scales.

The time resolution of the CCD is governed by the integration time between successive CCD read-outs, i.e., the frame-time τ. The specification of the spatial resolution element is more difficult to characterize because, in addition to the physical pixel size, it involves the detailed physics of how the charge-clouds created by the photons overlap, as well as the details of the event-detection algorithm. Unfortunately, a charge cloud created by an X-ray photon is not generally confined to the pixel where the charge-cloud originated. Hence, event-detection involves the examination of the pixel of the candidate event as well as its neighboring pixels. For the Chandra ACIS CCDs, the most commonly used event-detection scheme involves the examination of 3 by 3 pixel cells. Such a region is called an *event-detection cell*. Its size specifies the fundamental spatial scale for pile-up effects.

The energy resolution of the CCD for single photon events may be described by a response function[3] $R(h, E)$ that gives the probability for a photon of energy E interacting with the CCD to produce a pulse-height h. Following Ref. 1, the two-photon response function $R(h, E_1, E_2)$ will be assumed to approximately obey the superposition condition

$$R(h, E_1 + E_2) = \sum_{h'<h} R(h', E_1) R(h - h', E_2). \tag{17}$$

A similar equation exists for the n photon case. In simple terms, the above equation means that the response of the detector to two piled photons will be the same as that produced by a single photon whose energy is the combined energy of the two photons.

The superposition hypothesis has two important ramifications. First of all, consider the pile-up of a first-order diffracted photon of energy E with a photon from the mth order. For a small enough bin-size $\Delta\theta$, it follows from the grating equation that the mth order photon will have an energy near mE. Hence, the superposition hypothesis implies that the energy of the combined event will be approximately $(m + 1)E$. That is, the event will look like one produced by diffracted photon from the $(m + 1)$th order.

The second important implication of the superposition hypothesis concerns the order-sorting process. Recall from the previous section that if the CCD has sufficient spectral resolution, one may apply the appropriate pulse-height filter to extract mth order events. This means that when applied to extract first order events, the filter will exclude events that are a result of pile-up because the piled events will look like higher order events. Plus and minus first orders are rather special in this regard. When a pulse-height filter is applied to pick out higher order events, e.g., second order, there is the possibility for the unwanted inclusion of events produced by the pile-up of lower order photons.

As a result, the observed count-rate for the first order diffracted spectrum will be lower than expected in the absence of pile-up. Hence, a pile-up model for the correction of the first order spectrum can be constructed by simply computing the probability of getting a single, unpiled first order event. For if pile-up did occur, such an event would not appear in the order-sorted first order spectrum.

There are two ways for pile-up to remove events from the first order diffracted spectrum. The first and most important way is from pile-up of other first order photons. The second way is through the pile-up of higher energy, higher order photons. The relative importance of these mechanisms may be ascertained by inspecting the ratio of the expected count rate of higher-order events in detection cell, to that of first order events in the same detection cell, in the absence of pileup. This ratio, expressed as

$$\frac{\sum_{m>1} (1/m) A^{(m)}(\lambda/m) s(\lambda/m)}{A^{(1)}(\lambda) s(\lambda)}, \tag{18}$$

is plotted in Fig. 1, assuming effective areas appropriate for the Chandra Medium Energy Grating (MEG) and evaluated for a constant value of $s(\lambda)$, and a power-law with a spectral index of 2. This figure shows that higher-order pile-up is important only at large wavelengths, and only then when the flux at large wavelengths is

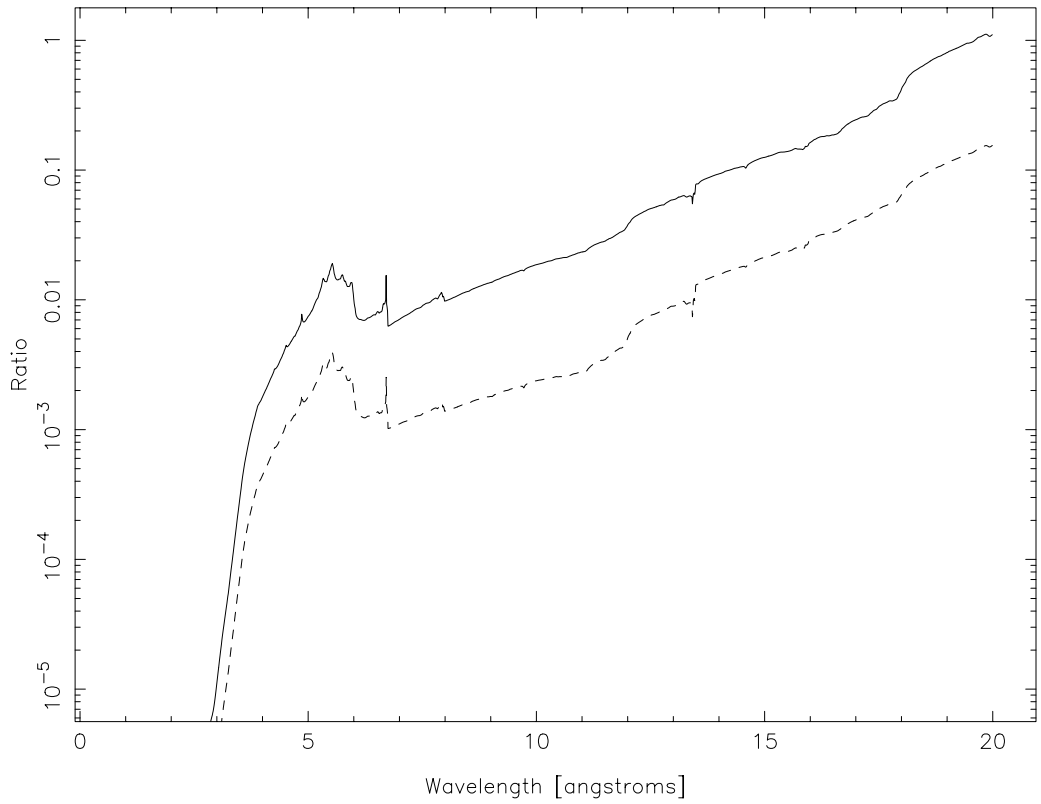

Figure 1. Figure showing the ratio of Eq. 18 of the expected count rate of higher-order events in a pixel, to the rate of first order events in the same pixel computed assuming no pileup. The solid curve shows the ratio evaluated for a constant value of $s(\lambda)$ using effective areas appropriate for the Chandra MEG. The dashed curve was generated assuming a power-law with a spectral index of 2. Although the ratio dominates at long wavelengths, first-order pile-up is not expected to be important there except for extremely bright sources.

large enough to cause pile-up in that region of the spectrum. For most astrophysical X-ray sources, this is rarely the case. For this reason, in what follows, only the channel involving the pile-up of first order photons will be considered. For notational simplicity, the first order effective area $A^{(1)}(\lambda)$ will be written simply as $A(\lambda)$.

It will be assumed that the diffracted spectrum is binned using a $\Delta\theta$ corresponding to the local wavelength equivalent of a CCD pixel. The cross-dispersion extraction width is assumed to be large enough to include a substantial fraction of the events, but not so large that background events become important. Furthermore, each of the bins Ω_i is assumed to consist of a central region where the incident flux may be great enough for pile-up to occur. Outside the pile-up region, the standard model described in the previous section will be used. For simplicity in what follows, the central pile-up region will be taken to have a cross-dispersion width of 5 pixels. Hence, the problem becomes that of finding the expected number of single-photon events that fall within the central 5 pixel pile-up region, under the event-detection constraint that a second photon cannot fall into the nearest neighboring pixels surrounding the first.

An important quantity governing the expected count rate is the amount of photon flux falling into each of the pixels. Let ω_{ij} denote the jth pixel in the ith extraction bin. Following the discussion of section 2, the flux F_{ij} of event-producing first order photons intercepted by this region is given by

$$F_{ij} = \int \mathrm{d}\lambda \; G^{(1)}_{\omega_{ij}}(\lambda) A(\lambda) s(\lambda), \tag{19}$$

where

$$G^{(1)}_{\omega_{ij}}(\lambda) = \int_{i\Delta\theta}^{(i+1)\Delta\theta} \mathrm{d}\theta \int_{z_j}^{z_{j+1}} \mathrm{d}z\, \mathcal{G}^{(1)}(\theta, z, \lambda). \tag{20}$$

Due to the sharp-peaked nature of $G^{(1)}_{\omega_{ij}}(\lambda)$, only a narrow range of wavelengths $\Delta\lambda$ centered upon $\lambda_i^{(1)}$ (cf. Eq. 14) will contribute to the integral over λ. With the assumption that $\Delta\lambda$ is small, Eq. 8 may be used to produce

$$F_{ij} = f_{ij} A_i s_i \Delta\theta, \tag{21}$$

where

$$f_{ij} = f^{(1)}(\lambda_i^{(1)}; z_j, z_{j+1}) \tag{22}$$

represents the cross-dispersion EEF for the jth pixel of the ith bin.

Assuming that the photon arrival times are Poisson-distributed, the probability for n photons to to interact with a pixel (i, j) during a time τ is given by

$$\frac{(\tau F_{ij})^n}{n!} \exp(-\tau F_{ij}). \tag{23}$$

To calculate the expected first-order count rate, it is simply a matter of enumerating the various possibilities for single photon events and then use Poisson statistics to assign a probability to each one. Fig. 2 shows the various combinations of the one and two single-photon event patterns that are considered.

The first possibility illustrated in Fig. 2 is that of a single photon in the center of the extraction region. Note that in accordance with the event detection scheme, no X-ray photon can interact with the 8 nearest neighboring pixels during the CCD frame. In addition the pattern excludes photons from the 4 pixels that are immediately adjacent to the neighboring pixels from the same row or column as the central pixel. The reason for this is as follows: The event detection scheme permits so-called "overlapping events", where two events share a subset of their respective nearest neighboring pixels. Some of liberated charge in the overlapping events may be counted twice causing an increase in the pulse-height of each of the events over what the pulse-height would be in the absence of the other event. In other words, overlapping events are another form of pile-up. Treating such events properly would require what are known as energy-dependent grade branching ratios. In the absence of such information, overlapping events will be treated in a purely ad-hoc manner by allowing diagonal overlapping events but not allowing overlapping events in the same row or column. Hence, in addition to requiring that the eight neighboring pixels be free of photon interactions, the pixels next to the nearest neighbors in the same row or column as the central event will also be required to be free of photon interactions.

As the reader can show, the probability for the first pattern of Fig. 2 is given by

$$\mathcal{P}_i^{(a)}(s_i) = \tau A_i s_i \Delta\theta f_{i0} e^{-\tau A_i s_i \Delta\theta (2f_{i2} + 6f_{i1} + 5f_{i0})}, \tag{24}$$

where for simplicity symmetry about $j = 0$ has been assumed such that $f_{i,-j} = f_{i,j}$. In addition, the flux in the neighboring bins at $i \pm 1$ was taken to be the same as the ith bin, i.e., $f_{i\pm1,j} = f_{i,j}$. Similarly, one can show that the probabilities associated with (b), (c), (d), and (e) of Fig. 2 are given by

$$\begin{aligned}
\mathcal{P}_i^{(b)}(s_i) =& \tau A_i s_i \Delta\theta f_{i2} e^{-\tau A_i s_i \Delta\theta (f_{i0} + 3f_{i1} + 5f_{i2} + 3f_{i3} + f_{i4})} \left[1 - \tau A_i s_i \Delta\theta (f_{i1} + f_{i2}) e^{-3\tau A_i s_i \Delta\theta (f_{i1} + f_{i2})}\right], \\
\mathcal{P}_i^{(c)}(s_i) =& \tau A_i s_i \Delta\theta f_{i1} e^{-\tau A_i s_i \Delta\theta (3f_{i0} + 6f_{i1} + 3f_{i2} + f_{i3})} \left[1 - \tau A_i s_i \Delta\theta f_{i2} e^{-\tau A_i s_i \Delta\theta (2f_{i1} + 3f_{i2} + 3f_{i3})}\right], \\
\mathcal{P}_i^{(d)}(s_i) =& (\tau A_i s_i \Delta\theta f_{i2})^2 e^{-\tau A_i s_i \Delta\theta (f_{i0} + 6f_{i1} + 10f_{i2} + 6f_{i3})},
\end{aligned} \tag{25}$$

and

$$\mathcal{P}_i^{(e)}(s_i) = (\tau A_i s_i \Delta\theta)^2 f_{i1} f_{i2} e^{-\tau A_i s_i \Delta\theta (3f_{i0} + 8f_{i1} + 8f_{i2} + 4f_{i3} + f_{i4})}, \tag{26}$$

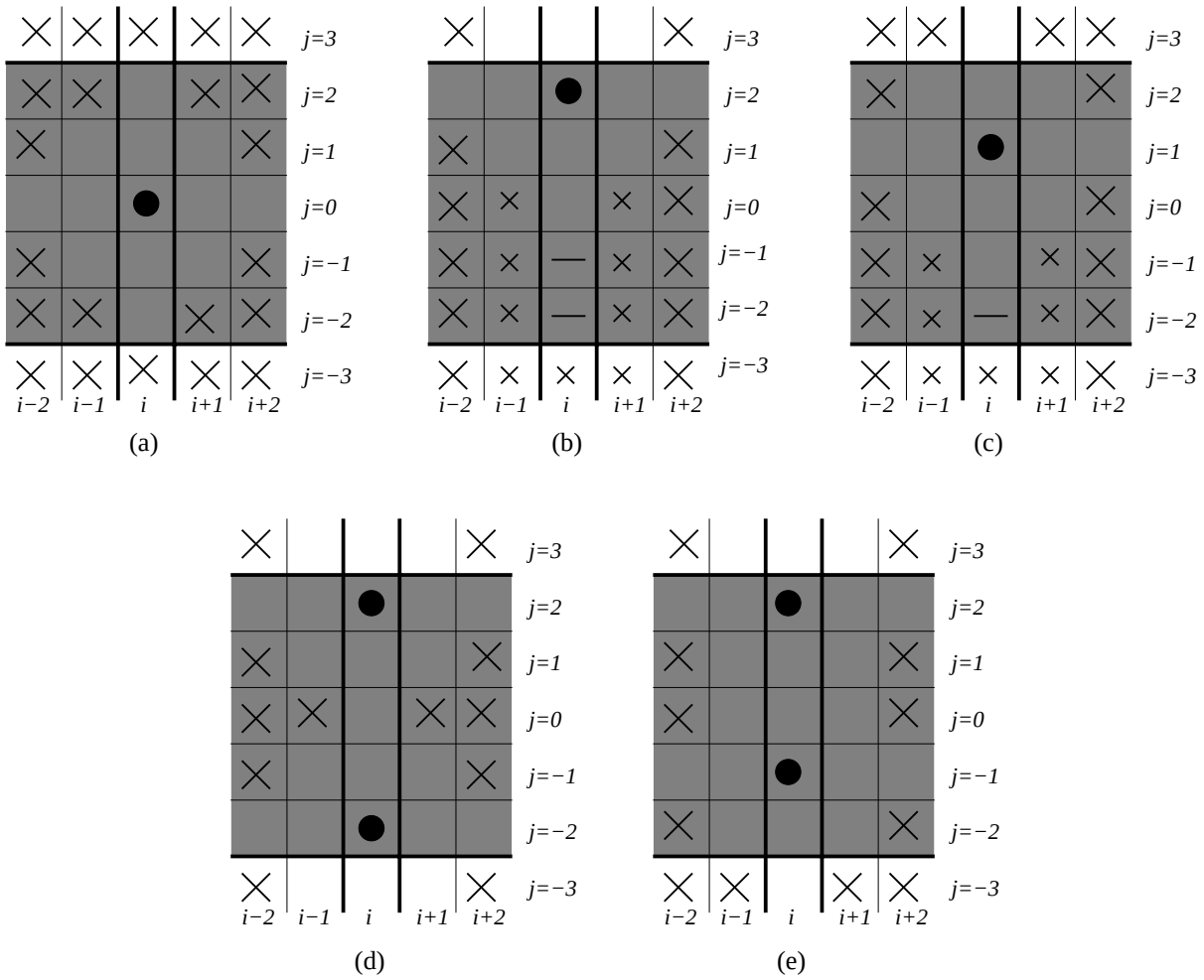

Figure 2. This figure illustrates the various event combinations in the central 5 pixel region of the ith bin. Pixels containing the solid circle involve the interaction of a single photon. Empty pixels represent those with no photon interactions. Pixels containing the large "X" denote pixels where the number of photon interactions are not important for the probability associated with the pattern. Pixels marked with a "–" contain no first order events, either because no photons interacted with the pixel, or because a second photon interacted in the pixel or one of its nearest neighboring pixel causing the event to be interpreted as one of higher order. The pixels marked with a small "x" are neighbors of those marked with a "–", and must be taken into account when computing the probabilities associated with those marked by a "–". Note that patterns obtained by the reflections (b), (c), and (e) via the operation $j \longrightarrow -j$ are not shown. See the text regarding the treatment of the next-nearest neighbors of an event, e.g., the $i+2$, $j=0$ pixel of (a).

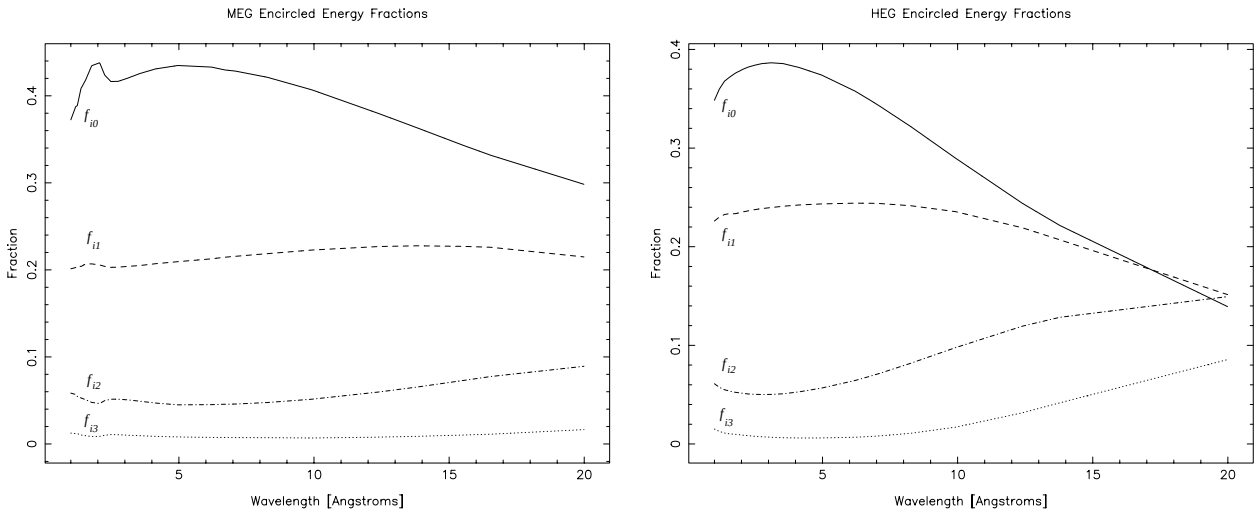

Figure 3. This figure shows plots of the encircled energy fractions used in the analysis. The left plot shows the encircled energy fractions for the MEG first order dispersion arm, and the plot at the right shows the fractions for the HEG arm.

respectively. In terms of these probabilities, the expected number of first-order events per frame in the ith bin is given by

$$\frac{C_i}{N} = [1 - f_{i0} - 2(f_{i1} + f_{i2})]\tau A_i s_i \Delta\theta + \mathcal{P}_i^{(a)}(s_i) + 2[\mathcal{P}_i^{(b)}(s_i) + \mathcal{P}_i^{(c)}(s_i)] + 2[\mathcal{P}_i^{(d)}(s_i) + 2\mathcal{P}_i^{(e)}(s_i)], \qquad (27)$$

where the first term represents the contribution from events falling outside the 5 pixel central pile-up region.

Equation 27 is the main result of this work. It relates the expected number of first-order events per frame in a wavelength bin to the incident source flux. Flux-correction within this model is achieved by solving the above equation for s_i given the observed first order spectrum C_i. This model has been implemented in the ISIS[4] spectral modeling program, which was used for the analysis of 4U 1636-53.

4. APPLICATION TO 4U 1636-53

The bright X-ray binary 4U 1636-53 was observed September 20, 1999 by the Chandra X-ray Observatory using the High Energy Transmission Grating (HETG) in conjunction with the ACIS-S CCD detector. The total duration for the observation was 32270 seconds using a 3.2 second frame-time.

Data were processed using standard CIAO 2.2 tools supplemented by custom software. Level 1 files were used with standard grade filtering applied. However, events that were flagged as so-called cosmic ray afterglow events were kept because of their misidentification for even moderately bright sources. Data were extracted for the MEG$\pm$1, MEG$\pm$3, and HEG$\pm$1 orders.

The ISIS spectral analysis program was used to analyze the data using the pile-up model presented in the previous section. The data used for the encircled energy fractions f_{ij} were extracted from the Chandra LSF data products, which were derived from MARX simulations. Plots of the encircled energy fractions are shown in Fig. 3.

Fig. 4 shows a plot of the MEG+1 and HEG+1 spectra corrected using the standard technique of section 2. Also shown on this plot as the solid curve is the MEG plus third order spectrum, which is believed to be free of pile-up for wavelengths greater than 4 angstroms. Most of the MEG third order data below 3Å are a result of 3 photon pile-up from MEG first order. Note that the HEG+1 flux-corrected spectrum appears to be consistent with the MEG third order spectrum beyond 6Å. However, the MEG first order spectrum does not agree with either of the other spectra over much of the wavelength range.

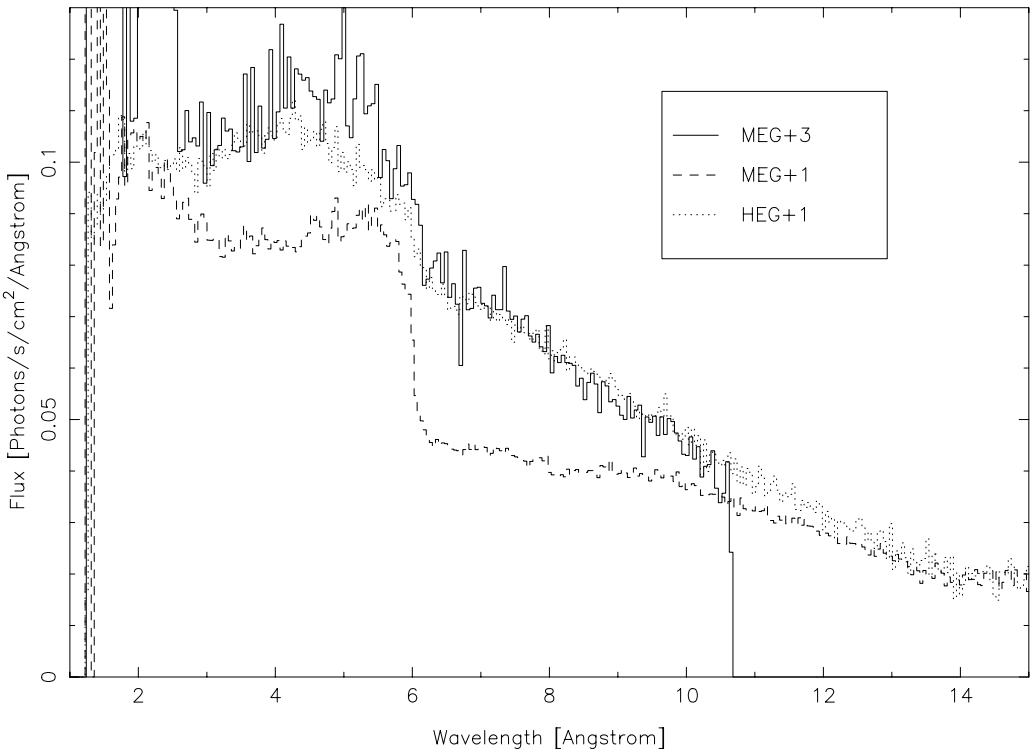

Figure 4. Figure showing the results of flux-correcting the 4U 1636-53 data using the standard flux correction technique based upon equation Eq. 16. As can be plainly seen, the standard approach fails to correct the MEG first order over much of the displayed wavelength band.

Flux-correction using the pile-up model of section 3 produces spectra that are in much better mutual agreement as shown in Fig. 5. As the figure shows, the MEG+1 and MEG+3 spectra agree quite well above about 5.5Å. Note that the pile-up correction has also increased the HEG first order spectrum so that it is systematically larger that the other two spectra above 6Å. It is easy to see that such an increase should be expected from a simple statistical argument. About 8 percent of the CCD frames contained an event in an event detection cell centered upon 8Å in the HEG+1 dispersion arm. This rate represents the fraction of observed single photon events, and does not include events due to multiple photons. From the application of Poisson statistics, it follows that the actual rate should be 8.7 percent in the absence of pile-up– a value that is about 9 percent larger.

There are several possible reasons for the differences between the different flux-corrected spectra. The most obvious one is the possibility of systematic errors in the calibration data, e.g., the effective areas. Also, simply increasing the encircled energy value f_{i1} by 5 percent can explain much of the difference between the MEG and HEG spectra. Other sources of error include the order-sorting tables used to extract first order events. These tables are made from the CCD redistribution matrices, which are known to be problematic above 7Å. In light of these considerations, the pile-up correction appears to be working well.

5. SUMMARY

In this paper a method of flux-correction applicable to grating data affected by pile-up was given. The effectiveness of the model was demonstrated by its application to the Chandra HETGS observation of 4U 1636-53.

The grating pile-up model as given in Eq. 27 has been implemented in the ISIS spectral modeling program. As such, one is not limited to simple flux-correction as was done for 4U 1636-53. One can also use ISIS to fit a spectral model to grating data affected by pile-up.

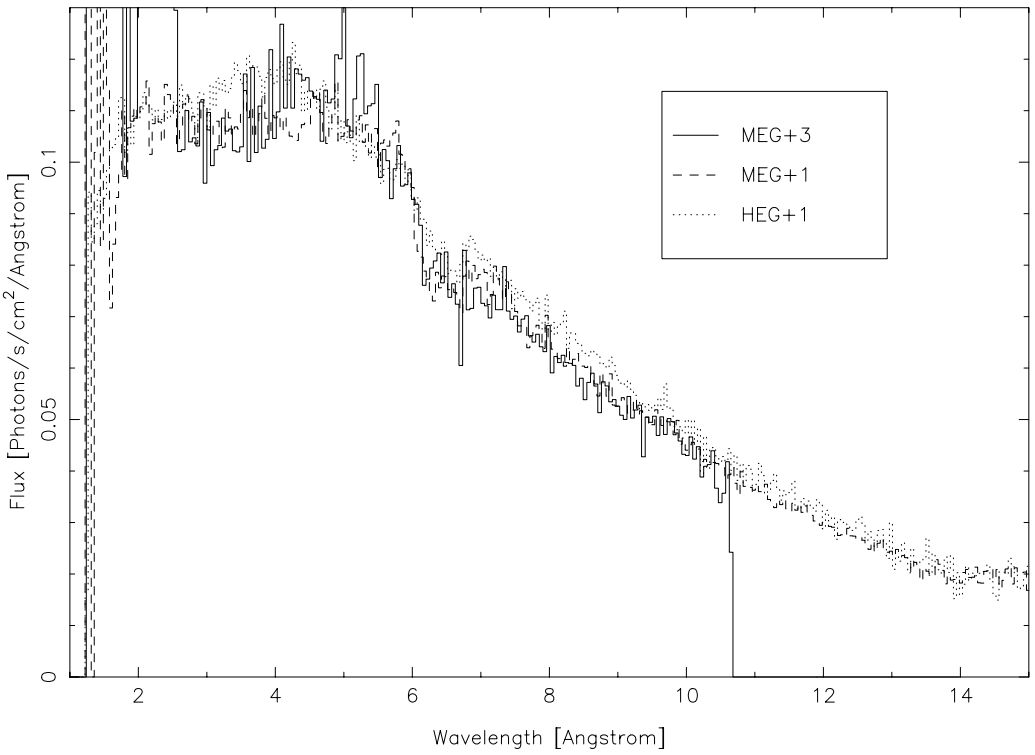

Figure 5. Figure showing the results of flux-correcting the 4U 1636-53 data using the pile-up model of Eq. 27. The flux-corrected HEG first order spectrum is systematically larger than the other two spectra. It is believed that this discrepancy is due to uncertainty in one or more of the calibration parameters.

More work still remains to be done. For example, preliminary tests with extremely bright sources such as Cygnus X-1 indicate that while the model works well on some parts of the spectrum, it needs to be improved in certain wavelength ranges where the amount of pile-up is severe. For such sources, pile-up is probably occurring outside the central 5 pixel region assumed in this work. Work is currently in progress to extend the model to an arbitrarily wide region. Nevertheless, it is hoped that the model described here will be sufficiently useful for a wide range of sources.

ACKNOWLEDGMENTS

I would like to thank Herman Marshall and Norbert Shultz for useful discussions about grating pile-up. I am grateful to Dan Dewey, David Huenemoerder, Herman Marshall, and Norbert Shultz for for their expert insight into Chandra calibration issues. Special thanks go to Glenn Allen who was especially helpful in diagnosing processing errors in the level 1 data, and to Bish Ishibashi for providing me with updated encircled energy fractions. Finally, I am indebted to John Houck for his help with ISIS and providing the appropriate hooks to permit the implementation of the model in a straightforward manner. This work was supported under Chandra X-Ray Center contract SV1-61010 from the Smithsonian Institution.

REFERENCES

1. J. E. Davis, "Event Pileup in Charge-coupled Devices," *ApJ* **562**, pp. 575–582, Nov. 2001.
2. M. C. Weisskopf, H. D. Tananbaum, L. P. Van Speybroeck, and S. L. O'Dell, "Chandra X-ray Observatory (CXO): overview," in *Proc. SPIE Vol. 4012, p. 2-16, X-Ray Optics, Instruments, and Missions III, Joachim E. Truemper; Bernd Aschenbach; Eds.*, **4012**, pp. 2–16, July 2000.

3. J. E. Davis, "The Formal Underpinnings of the Response Functions Used in X-Ray Spectral Analysis," *ApJ* **548**, pp. 1010–1019, Feb. 2001.
4. J. C. Houck and L. A. Denicola, "ISIS: An Interactive Spectral Interpretation System for High Reso lution X-Ray Spectroscopy," in *ASP Conf. Ser. 216: Astronomical Data Analysis Software and Sy stems IX*, **9**, pp. 591+, 2000.